Photochemistry and Photobiology, 2006, 82: 373–379

Symposium-in-Print: Green Fluorescent Protein and Homologs

Time-Resolved Emission Spectra of Green Fluorescent Protein

Andrew A. Jaye[1,2], Deborah Stoner-Ma[2], Pavel Matousek[3], Michael Towrie[3], Peter J. Tonge[2] and Stephen R. Meech*[1]

[1]School of Chemical Sciences & Pharmacy, University of East Anglia, Norwich, NR4 7TJ, England
[2]Department of Chemistry, Stony Brook University, Stony Brook, NY 11794-3400
[3]CCLRC Central Laser Facility, Rutherford Appleton Laboratory, Chilton, Didcot, Oxfordshire, OX11 0QX, England

Received 7 May 2005; accepted 17 August 2005; published online 23 August 2005 DOI: 10.1562/2005-05-07-RA-518

ABSTRACT

The time-resolved emission spectra of wild-type green fluorescent protein (wtGFP) and the T203V GFP mutant have been recorded with picosecond time resolution, allowing the separate characterization of the two spectral components associated with the neutral and anionic forms of the GFP chromophore. Significantly, neither component shifts as a function of time. It is suggested that the absence of spectral shift is a result of highly restricted movement of the protein residues in the vicinity of the chromophore. The shapes of the separated spectra are discussed and their relative ratio analyzed in a steady-state analysis.

INTRODUCTION

The intrinsically fluorescent green fluorescent protein (GFP) has found very widespread application in bioimaging (1,2). Fusions of the gene for GFP with that of a target protein lead to the target being expressed irreversibly bound to GFP. A posttranslational cyclization and oxidation reaction among three adjacent amino-acid residues forms the chromophore and renders GFP, and thus the target protein, strongly fluorescent, without the addition of any cofactors (1,2). Because of its importance, and the need to produce mutants with specific properties such as pH or ion-sensing capabilities, there has been intense interest in understanding and controlling the excited-state chemistry of GFP (3–15).

The electronic spectrum of wild-type GFP (wtGFP) reveals that the ground state of the chromophore exists in two forms, protonated (neutral), yielding the A form of the protein, and deprotonated, giving the anionic B form (3,4,16). The relative populations of the A and B forms are insensitive to pH in wtGFP, but can be modulated by introducing site-specific mutations in and around the chromophore. These mutations not only change the relative populations of the two chromophore forms, but also affect the absorption and emission properties of the chromophore while rendering it sensitive to pH. On excitation of the neutral A form in wtGFP, the A* state undergoes a rapid (tens of picoseconds) excited-state proton transfer reaction to form an anionic (I*) form, which emits the dominant green-yellow GFP fluorescence with a nanosecond lifetime and 80% quantum efficiency (1,2). Once in the I ground state, the proton has been observed to return to the chromophore reforming the A ground state on multiple timescales in the picosecond range (17). The A* emission is seen only as a very weak shoulder on the I* peak in the steady-state spectrum (3). The proton transferred from the A* state initiates an ultrafast proton relay reaction, involving an adjacent bound water molecule and two amino-acid residues, calculated (18) and observed (19) to result in the ultrafast protonation of a carboxylate residue, E222. The fluorescent I* state is similar to the B* state accessed directly from the B ground state, but exists in an unrelaxed protein environment. The conversion between the I and B states, which is believed to involve isomerization in the Thr203 residue, takes place on a much slower timescale (20). These structural changes are summarized in Fig. 1.

In contrast to the high fluorescence quantum yield of the intact protein, the denatured protein is essentially nonfluorescent (21). Model compounds of the GFP chromophore have been synthesized, and were also found to be nonfluorescent at room temperature, although fluorescence is restored on freezing in a glass to 77 K (22,23). The mechanism of radiationless decay in the chromophore has been studied in considerable detail (24–31). It was found that the excited state decays through a rapid internal conversion, which exhibits only a weak dependence on medium viscosity. It was proposed that the mode (or modes) coupling the excited state to the ground state is (are) volume conserving, and the barrier to reaction is low (near zero at 295 K) (26–28). One unresolved question in GFP photophysics lies in understanding how the protein effectively suppresses such an efficient radiationless decay channel. Certainly, the enhancement of the fluorescence channel suggests an important role for protein–chromophore interactions. In this work we investigate the time dependence of the fluorescence spectra of wtGFP and a GFP mutant, T203V, in which the key threonine depicted in Fig. 1 is replaced by a valine, thereby destabilizing the anionic form of the chromophore and favoring the neutral form. The time dependence of the fluorescence spectrum is expected to be a sensitive probe of the evolution of chromophore–environment interactions.

*Corresponding author email: s.meech@uea.ac.uk (Stephen R. Meech)
© 2006 American Society for Photobiology 0031-8655/06

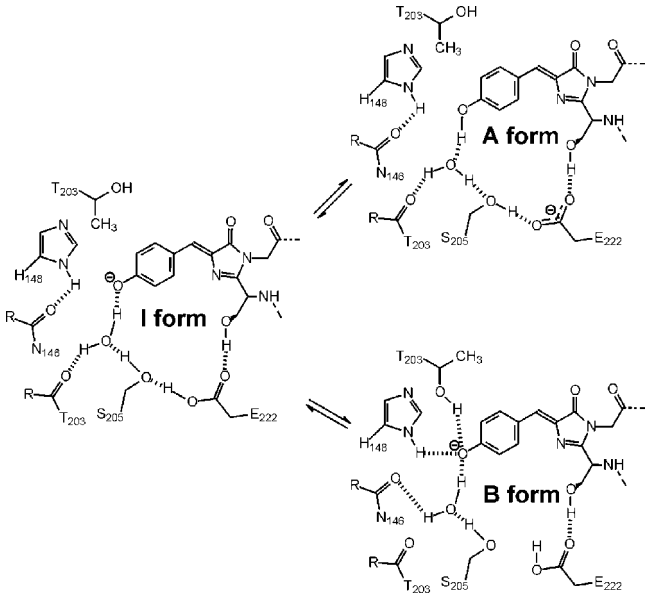

Figure 1. The A*, I* and B* states of GFP (adapted from Brejc *et al.* [16]).

MATERIALS AND METHODS

Measurements of the time-resolved fluorescence spectra were made with the use of a Kerr gated spectrometer described in detail elsewhere (32). The laser source is an amplified ultrafast titanium sapphire laser. The output at 800 nm (up to 3 mJ/pulse in 150 fs at a repetition rate of 1 kHz) is routed through a thin BBO crystal to generate 400 nm pulses, resonant with the A–A* transition of wtGFP and T203V. The excitation pulses are routed through a $\lambda/2$ plate to adjust the polarization to the magic angle. The pulse energy is attenuated to $\sim$ 0.04 μJ/pulse and focused into the sample cell with a spot diameter of 300 μm. The cylindrical cell has a path length of 2 mm and could be translated and spun to minimize sample damage. The fluorescence from the sample cell is collected and focused into the Kerr cell that comprises a pair of crossed polarizers around a cell containing carbon disulfide as the Kerr medium. With the polarizers crossed, no fluorescence is transmitted through the cell. However, when the CS_2 is illuminated with an intense pulse (the residual 800 nm radiation), a large transient birefringence is produced. During the lifetime of the birefringence the Kerr cell is open and fluorescence is transmitted. The fluorescence is dispersed in a polychromator and measured with a multichannel detector. Varying the time delay between the excitation and gate pulses controls the timing of the spectrum. With the use of this method a set of time-resolved spectra are collected in a few minutes with a spectral resolution of 4 nm. Data collection is faster and spectral resolution higher than with the alternative technique of fluorescence upconversion and spectral reconstruction (33), although the time resolution is lower (4 ps), because of dispersion in the Kerr gate and the finite response time of the Kerr medium. The spectra presented below are uncorrected for the wavelength-dependent sensitivity of the detection system.

wtGFP was overexpressed in *Escherichia coli* as a His-Tag construct and purified with the use of NiNTA (Novagen, Madison, WI) affinity chromatography. Protein was eluted from the NiNTA column with 100 m*M* imidazole buffer, dialyzed into 20 m*M* potassium phosphate pH 7.5, 200 m*M* NaCl, and concentrated to approximately 100 μ*M* with the use of a Centricon YM10 filtration unit (Millipore Corp., Bedford, MA).

The T203V GFP mutation was introduced with the use of the QuikChange mutagenesis kit (Stratagene, LaJolla, CA). Mutant protein was expressed and purified as for wtGFP. Both proteins showed a dominant absorbance peak at roughly 400 nm.

Steady-state fluorescence spectra were recorded on a Fluorolog-3 fluorimeter (Jobin Yvon-Spex, Edison, NJ). Absorbance spectra were recorded on a Cary 100 Bio UV-visible spectrophotometer.

RESULTS AND DISCUSSION

The time-resolved emission spectra for wtGFP and T203V are shown in Fig. 2. The decrease in the A* intensity and associated

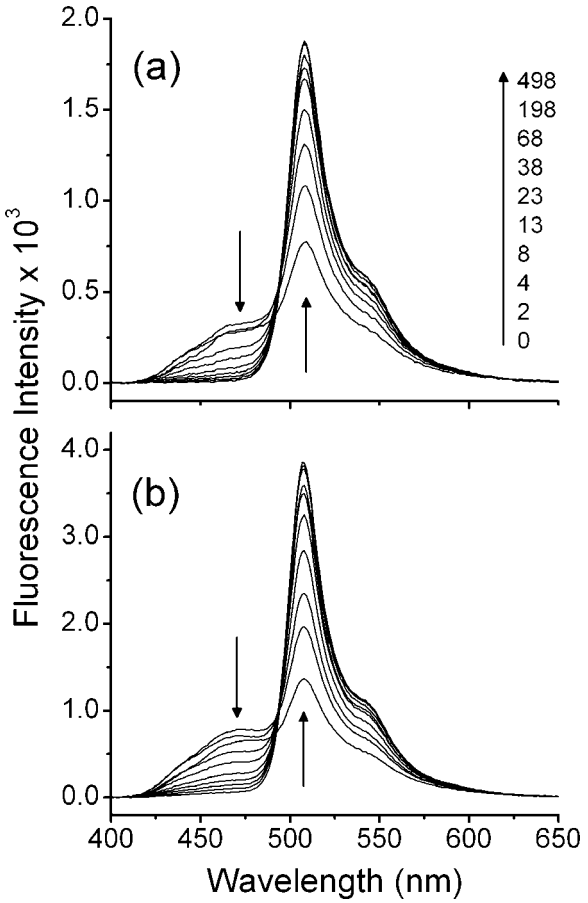

Figure 2. Picosecond time-resolved emission spectra for (a) wtGFP and (b) T203V measured with the Kerr gate method (see text for details). The key shows pump-gating pulse time delays in picoseconds for both (a) and (b); the arrows show the direction of change with increasing time.

increase in the I* intensity with increasing time after excitation are evident. These time-dependent intensity changes are assigned to the excited-state proton transfer reaction (3,4). The clear isoemissive points at 488 $\pm$ 5 nm for both wtGFP and T203V suggest the existence of only two emissive states. It is also apparent that a significant population is formed in I* promptly, that is, within the 4 ps time resolution. The extent to which this is due to the fastest component of the proton transfer reaction or to the cross-well excitation (direct population of I* from A) identified in transient absorption by Winkler *et al.* (13) cannot be assessed from our data, due to the limited time resolution. However, the ratio of I*/A* emission at $t \approx 0$ is in reasonable agreement with the transient absorption data (13).

The main interest in the current work is in the time dependence of the spectra. However, kinetic information (time-dependent intensity at a fixed wavelength) can also be determined from the same data set. Kinetic data at 474 and 508 nm are shown in Fig. 3 for wtGFP (Fig. 3a) and T203V (Fig. 3b). The fluorescence decay kinetics of these two variants have been reported previously (6), and were found to be of multiexponential character. The present kinetic data are compared with the earlier measurements of Kummer *et al.* (6), convoluted with the 4 ps response time of the Kerr gate spectrometer. As can be seen in Fig. 3, the agreement between our experimental data and that of Kummer *et al.* is excellent.

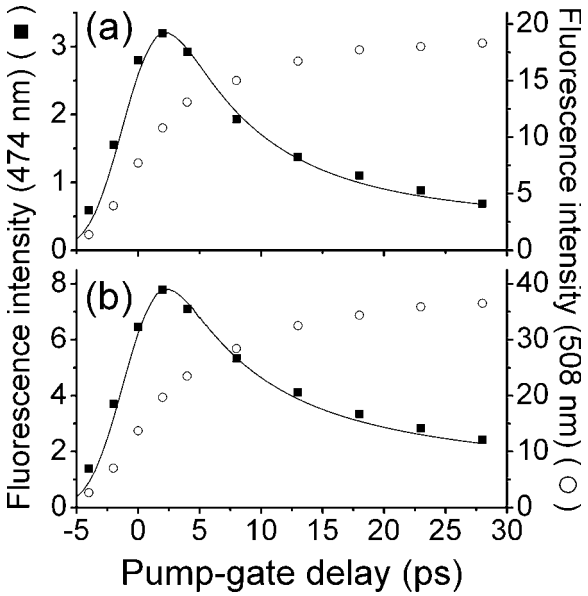

Figure 3. Kinetic data for (a) wtGFP and (b) T203V at 474 and 508 nm. The fitted lines to the 474 nm data are a convolution of the previously reported fluorescence decay (6) with the 4 ps instrument response of the Kerr gate spectrometer.

To further analyze the data, the spectra are separated into A* and I* components. Various separation methods have been attempted. Fitting to multiple Gaussian or log-normal peaks did not provide a unique or accurate fit. Because the spectra are reasonably well separated a more direct method was employed. The spectrum due to I* at long times, where the A* emission has decayed away, was multiplied by a constant factor (a) and subtracted from the measured time-resolved spectrum (F).

$$\mathrm{I}_{\mathrm{A}^*}(\lambda, t) = \mathrm{I}_{\mathrm{F}}(\lambda, t) - a\mathrm{I}_{\mathrm{I}^*}(\lambda, t = \infty)$$

The result of the subtraction is the A* emission, isolated from I*. The A* emission spectrum (Fig. 4) is very broad, extending beyond 600 nm, that is, underlying the entire I* emission. The isolated A* spectra are perturbed by a subtraction artifact at the peak of the I* emission. The size of the artifact was minimized by adjusting the fitting parameter, a.

To eliminate the artifact in subsequent analysis the $\mathrm{I}_{\mathrm{A}^*}(\lambda,t)$ were fit to an extreme exponential line shape

$$\mathrm{I}_{\mathrm{A}^*}(\lambda, t) = \mathrm{A}\exp(e^{-z} - z + 1),$$

in which

$$z = \frac{\lambda - \lambda_0}{\Delta\lambda/\sqrt{2\pi}}$$

where λ_0 is the maximum and $\Delta\lambda$ is the spectral width. This function gave a better fit than the more established log-normal function, perhaps indicating the unusually broad asymmetric nature of the spectrum. The time-dependent fit parameters are shown in Table 1. It is immediately apparent that the A* spectrum is independent of time. The fit to the A* spectrum can be subtracted from the total spectrum to isolate the I* emission. As could be inferred from the raw data and the existence of an isoemissive point (Fig. 2), the I* spectrum is also independent of time. The isolated I* spectra are shown in Fig. 5.

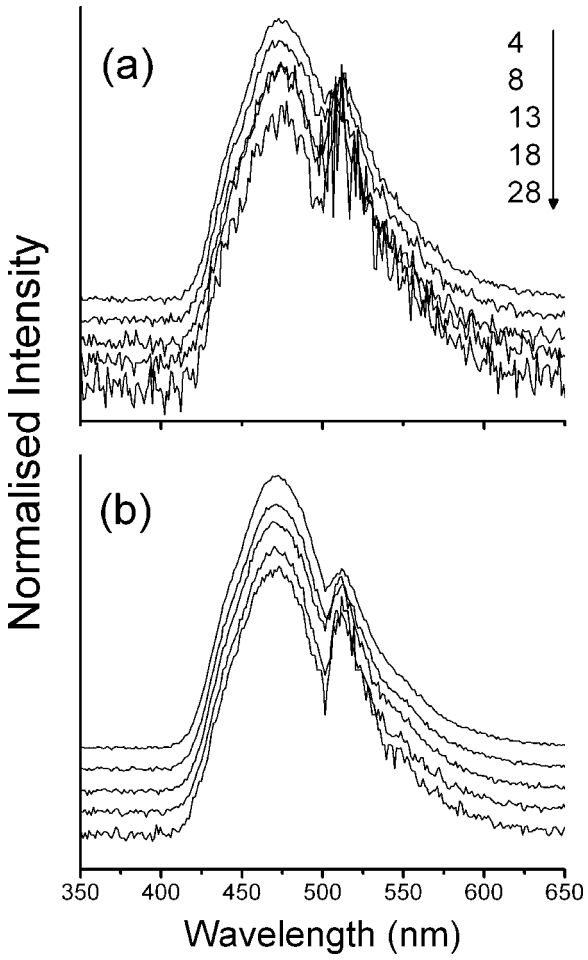

Figure 4. Time-dependent spectra of the A* state, offset and normalized for clarity (the feature around 495–515 nm is an artifact associated with the subtraction procedure). The key details the pump-gating pulse time delay of each spectrum given in picoseconds.

The first conclusion is that neither the A* nor the I* emission spectra exhibit any time dependence for either of the GFP mutants. This is an interesting and surprising result in the light of the observation by Stark-effect spectroscopy that the dipole moment of the chromophore changes markedly between excited and ground states (34). The observed change on excitation of the A → A* transition is 2.5 D, while that between B and B* is ca 7 D (34). Thus, each transition in the GFP photocycle (Fig. 1) is accompanied by an appreciable change in chromophore dipole moment. In fluid solution it is expected that the medium would relax in response to the changed electrostatic interaction between solvent and solute (35), leading to a continuous shift in the emission spectrum to lower energy (36). The rate of redshift of the emission spectrum of a solute can be related to the dynamics of the surrounding medium, such as the dielectric or Kerr relaxation times (37), whereas the magnitude of the shift depends on the magnitude of the dipole moment change and the dielectric properties of the medium. Such time-resolved fluorescence shifts have also been observed in several different protein environments including: intrinsic (tryptophan) amino-acid fluorescence (38); fluorescence from a synthetic amino acid incorporated at various sites in a protein (39); extrinsic probes adsorbed at either polar or nonpolar binding sites (40–42), although the latter is complicated by contact of probe molecules with the

Table 1. Parameters for fit of extreme exponential function to A* spectra shown in Figure 4.

	wtGFP			T203V		
Delay time (ps)	λ_0/nm	$\Delta\lambda$/nm	A	λ_0/nm	$\Delta\lambda$/nm	A
4	476.6	91.7	279	471.5	85.2	650
8	477.2	93.0	181	471.7	86.7	468
13	477.3	92.2	124	472.7	88.7	345
18	477.6	95.3	91	471.7	88.2	260
28	480.1	98.8	56	472.8	90.7	172

water environment (43). The absence of a measurable time-resolved shift in fluorescence for wtGFP and T203V, in either the A* or I* states, can be explained by one of two factors. First, the medium is unperturbed by the change in chromophore dipole moment (i.e., the chromophore–protein interactions are weak). Alternatively, the medium is so rigid that no relaxation occurs on the timescale of the excited-state lifetime, which reaches nanoseconds for the I* state. The similarity between the spectrum of the GFP chromophore in the protein and in the gas phase could support the idea of a weak interaction (44). However, both the dramatic enhancement of chromophore fluorescence by the protein and the fact that different mutants exhibit different spectral properties argue that the protein in fact has a strong interaction with the chromophore. Thus, the lack of a shift in response to the changed dipole moment of the chromophore on conversion to the I* state from the A* state, is more consistent with an environment in which reorientation of polar or polarizable residues in the vicinity of the chromophore are suppressed, due to the high rigidity of the protein environment. Having said this, we note that a rotation around the Thr203 residue does occur in wtGFP on conversion from I to the B state (20). This rearrangement is exhibited in the crystal structure of wtGFP decarboxylated at Glu222, in which only the anionic form of the chromophore is populated (45). Importantly, however, we do not observe any contribution from I/B interconversion in our fluorescence spectra, as this interconversion is not significant during the timescale of our measurements. In fact, we estimate from OD values that less than 10% of the sample is converted to the B form after 20 min of irradiation.

A final possibility is that the Stokes shift is too fast to be resolved within the 4 ps time resolution. This may be the case if the relaxation is dominated by subpicosecond inertial (librational) motion of the environment, while diffusive reorientation of the environment is suppressed. In the case of bacteriorhodopsin it was found that excited-state solvation was dominated by the inertial response, and the diffusive component was suppressed due to the constrained environment, as suggested above for GFP (46). We cannot rule out such a component with our current time resolution, but believe it to be relatively less significant in GFP, because of the overall smaller Stokes loss.

The second conclusion is that the A* and I* emission spectra have distinctly different shapes. I* is narrow and reveals clear vibronic structure at ca 1400 cm^{-1} with respect to the intense origin (Fig. 5), in agreement with previous reports (47). Close inspection of the A* band also reveals weak vibronic structure, but the spectrum is much broader and more asymmetric (Fig. 4). The A* vibronic structure reveals a similar wave number to I*, estimated to be 1500 ± 200 cm^{-1}, but its spectrum is poorly resolved, and the origin peak is not strong. In terms of a single coordinate description of these vibronic transitions, this result can be taken to indicate that

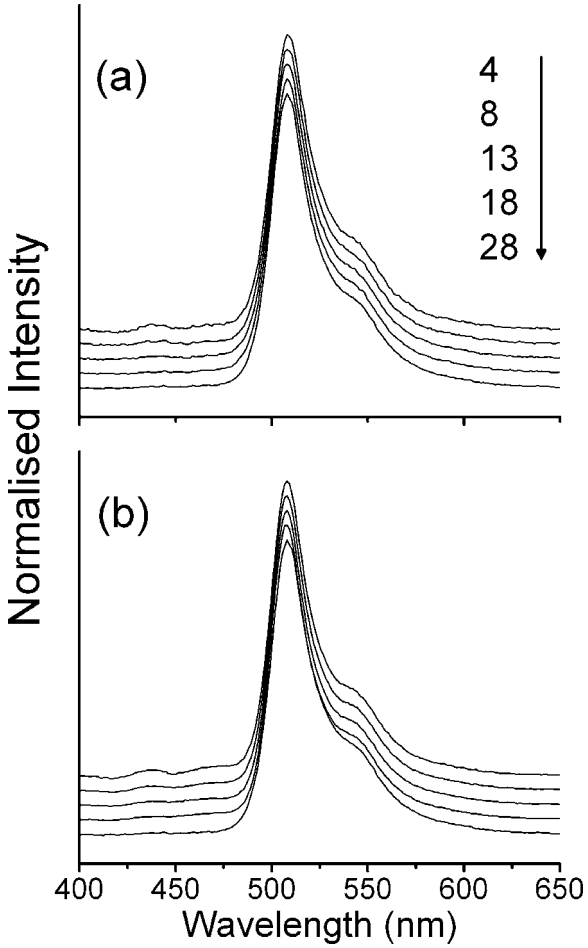

Figure 5. Time-dependent spectra of the I* state which have been offset for clarity. The key details the pump-gating pulse time delay of each spectrum given in picoseconds.

the A ← A* transition is displaced, i.e. the ground and excited states have different equilibrium structures, while the I ← I* transition is between structurally similar states. This picture is also obtained from the Stokes shifts, which are 60 and 8 nm, respectively (17). Although a single coordinate picture is certainly a great oversimplification of the GFP vibronic structure, it is noteworthy that the resonance and preresonance Raman spectra are dominated by a mode at 1565 cm^{-1} (48,49). A displaced coordinate for the A ← A* transition is consistent with the very broad and asymmetric form of the spectrum. The undisplaced character of the fluorescent I ← I* transition in GFP is one factor that distinguishes it from the very weakly fluorescent excited state of the model chromophore, 4′-hydroxybenzylidene-2,3-dimethylimidazolinone (HBDI) anion. The HBDI anion has a spectral profile that is quite similar to the neutral form of HBDI, but shifted to lower energy.

Finally it is noteworthy that the ratio $I_{A*}(t)/I_{I*}(t)$ is different between the two GFP mutants. The difference at time zero could be indicative of a different degree of cross well excitation, as discussed by Winkler et al (13). However, given that our time resolution is on the timescale of the fastest component in the proton transfer reaction, this may also reflect differences in the kinetics of the proton transfer reaction.

An alternative approach to understanding the contribution of A* emission to the spectrum is to conduct a steady-state analysis of the

Table 2. Relative intensity of A* and I* emission as a function of deuteration.

Protein	Solvent	$(I_{A^*}{}^a / I_{I^*}{}^b)/10^{-2}$	$(I_A/ I_{I^*})^c/10^{-2}$
GFP	H_2O	0.5	2.2
GFP	D_2O	1.7	10
T203V	H_2O	1.6	2.9
T203V	D_2O	3.1	—

[a]Determined at 450 and 460 nm.
[b]Determined at 509 and 511 nm for wtGFP and T203V, respectively.
[c]Ratio calculated according to Scheme 1. For rate constants see text.

I_{A^*} / I_{I^*} ratio. We have observed that the ratio is also a function of mutation and deuteration (Table 2, Fig. 6). The effect of deuteration is to enhance the ratio by a factor of 3 in wtGFP and 2 in T203V. Thus, the effect of deuteration is somewhat dependent on the particular mutant. It is also seen that the I_{A^*}/I_{I^*} ratio itself a function of the mutation, the relative contribution of A* emission being larger for T203V than wtGFP. We compare those observations with the predictions of the following simplified kinetic scheme (Scheme I) in which excited A* may relax via proton transfer to form I* or via vibrational relaxation to generate a form of A which does not undergo proton transfer, A^0. This simplified scheme reproduces the nonexponential decay of the A* emission. It can easily be extended to more realistic cases [as has been shown by Winkler (13)] but this is not required for a stationary state analysis. It is straightforward to show that under steady-state conditions scheme I leads to

$$\frac{I_A}{I_{I^*}} = \frac{k_I k_{FA}(k_{A^0} + k_{VR})}{k_{A^0} k_{FI} k_H},$$

where k_H is the proton transfer rate constant, $I_A = I_{A^*} + I_{A^0}$ and $k_A = k_{FA} + k_{NRA}$, $k_{A^0} = k_{FA^0} + k_{NRA^0}$, $k_I = k_{FI} + k_{NRI}$ and, as they are spectroscopically indistinguishable, $k_{FA} = k_{FA^0}$. An estimate of the ratio can be obtained by making reasonable assumptions about some of the rate constants. From the quantum yield and lifetime of the I* state, we can estimate the radiative rate k_{FI} as 0.19 ns^{-1}, and from the lower oscillator strength for A* ← A we estimate k_{FA} = 0.15 ns^{-1}. An estimate of the decay rate constants, k_I, is obtained from the measured fluorescence decay times in wtGFP and T203V, as 0.24 and 0.27 ns^{-1}, respectively. Similarly, to obtain k_{A^0} we assume that this reflects the hundreds of picoseconds components observed in A* fluorescence, yielding 5 ns^{-1}. The rate of vibrational relaxation is not measured for GFP, but based on measurements on polyatomic molecules in fluid solution 50 ns^{-1} may be assumed. Finally, to obtain an estimate of k_H, the proton transfer constant, the following procedure is used. For wtGFP and T203V the proton transfer rate constant is calculated from the weighted mean of the fast components of the A* fluorescence decay (6), where the long component is assumed to be associated with the decay of A^0, yielding 95 and 80 ns^{-1} for wtGFP and T203V, respectively. To obtain a value for deuterated GFP, we use the observed slowing of the proton transfer rate by a factor of 5 as reported by Chattoraj *et al.* (3).

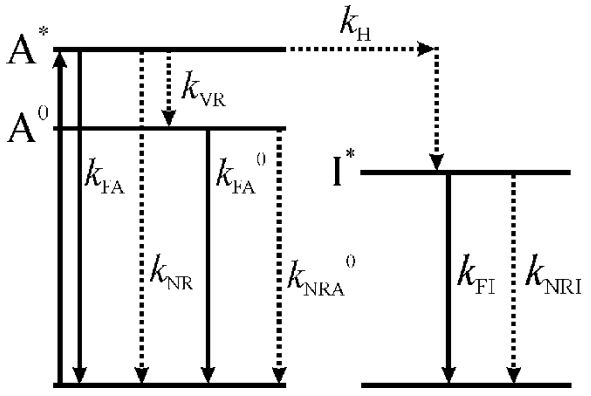

Scheme 1. Simplified kinetic scheme for GFP photophysics. F and NR indicate radiative and nonradiative rate constants, respectively, of states A, A^0 and I. k_{VR} is the rate constant for vibrational relaxation in A*, and k_H is the rate constant for proton transfer.

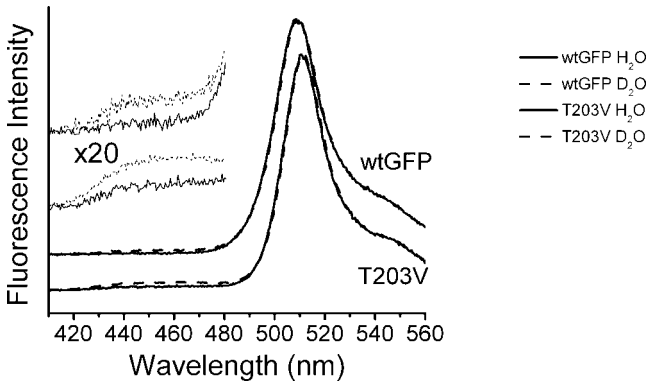

Figure 6. Stationary-state emission spectra of wtGFP, T203V (solid lines), deuterated wtGFP and deuterated T203V (dashed lines) normalized at the peak of the I* emission. The insets show the A* fluorescence.

The scheme correctly predicts the experimentally observed order for the I_{A^*}/I_{I^*} ratio: wtGFP < T203V < deuterated wtGFP. This indicates that the underlying kinetics are correctly contained within the scheme. However, the scheme fails rather badly in predicting the absolute ratio. One factor that is absent from Scheme 1 is the 'cross well' excitation, or direct excitation to I* at 400 nm. This omission will lead to an overestimation of the ratio, as observed. An alternative explanation is that the procedure used to calculate (and measure) k_H is inadequate. Agreement between the calculated and measured I_{A^*}/I_{I^*} ratio could be obtained by assuming that there are components in the proton transfer that are significantly faster than were considered or observed in the fluorescence experiments. These two explanations for the observed discrepancy are of course related, in the sense that cross-well excitation can be taken to correspond to infinitely fast components in the proton transfer reaction. The overestimation of the effect of deuteration on the ratio can then be understood on the basis that these ultrafast proton transfer rates are relatively less sensitive to deuteration than the slower components observed in fluorescence decay.

CONCLUSIONS

The time-dependent emission spectra of wtGFP and T203V have been recorded with the use of the Kerr gated technique. Simple subtraction procedures were used to separate the spectra due to A* from those due to I*. The width and very weak vibronic structure of the A* emission suggest a significant difference in structure between ground and excited electronic state. In contrast the I ← I* transition is characteristic of unshifted states of similar structure.

Neither spectrum shows any observable time dependence on the picosecond timescale. This result was discussed in terms of the known change in dipole moment between ground and excited states. It is suggested that the GFP chromophore sits in an environment in which reorientation of the adjacent polar or polarizable amino-acid residues is severely restricted, at least on the timescale of A* and I* state lifetimes. Finally, the dependence of the relative emission intensity I_{A*}/I_{I*} on mutation and deuteration has been studied in a steady-state analysis. A simple kinetic scheme has been given that reproduces the observations qualitatively but not quantitatively. It is suggested that the quantitative difference can be understood as arising from either cross-well excitation or an unresolved and deuteration-insensitive ultrafast proton transfer step.

Acknowledgements—This work was supported in the United Kingdom by grants from EPSRC and CCLRC and in the United States by NIH grant GM66818. P.J.T. is an Alfred P. Sloan Fellow. A.A.J. is grateful to EPSRC for a studentship.

REFERENCES

1. Zimmer, M. (2002) Green fluorescent protein (GFP): applications, structure, and related photophysical behavior. *Chem. Rev.* **102**, 759–782.
2. Tsien, R. Y. (1998) The green fluorescent protein. *Annu. Rev. Biochem.* **67**, 509–544.
3. Chattoraj, M., B. A. King, G. Bublitz and S. G. Boxer (1996) Ultra-fast excited state dynamics in green fluorescent protein: multiple states and proton transfer. *Proc. Natl. Acad. Sci. U.S.A.* **93**, 8362–8367.
4. McAnaney, T. B., E. S. Park, G. T. Hanson, S. J. Remington and S. G. Boxer (2002) Green fluorescent protein variants as ratiometric dual emission pH sensors. 2. Excited state dynamics. *Biochemistry* **41**, 15489–15494.
5. Lossau, H. S., A. Kummer, R. Heinecke, F. Pollingerdammer, C. Kompa, G. Beiser, T. Johnsson, C. M. Silva, M. M. Yang, D. C. Youvan and M. E. Michel-Beyerle (1996) Time-resolved spectroscopy of wild-type and mutant green fluorescent proteins reveals excited state deprotonation consistent with fluorophore-protein interactions. *Chem. Phys.* **213**, 1–16.
6. Kummer, A. D., J. Wiehler, H. Rehaber, C. Kompa, B. Steipe and M. E. Michel-Beyerle (2000) Effects of threonine 203 replacements on excited-state dynamics and fluorescence properties of the green fluorescent protein (GFP). *J. Phys. Chem. B* **104**, 4791–4798.
7. Kummer, A. D., C. Kompa, H. Lossau, F. Pöllinger-Dammer, M. E. Michel-Beyerle, C. M. Silva, E. J. Bylina, W. J. Coleman, M. M. Yang and D. C. Youvan (1998) Dramatic reduction in fluorescence quantum yield in mutants of green fluorescent protein due to fast internal conversion. *Chem. Phys.* **237**, 183–193.
8. Kummer, A. D., J. Wiehler, T. A. Schüttrigkeit, B. W. Berger, B. Streipe and M. E. Michel-Beyerle (2002) Picosecond time-resolved fluorescence from blue-emitting chromophore variants Y66F and Y66H of the green fluorescent protein. *ChemBioChem* **3**, 659–663.
9. Cinelli, R. A. G. (2001) Coherent dynamics of photoexcited green fluorescent proteins. *Phys. Rev. Lett.* **86**, 3439–3442.
10. Tozzini, V. and R. Nifosì (2001) *Ab initio* molecular dynamics of the green fluorescent protein (GFP) chromophore: an insight into the photoinduced dynamics of green fluorescent proteins. *J. Phys. Chem. B* **105**, 5797–5803.
11. Helms, V., C. Winstead and P. W. Langhoff (2000) Low-lying electronic excitations of the green fluorescent protein chromophore. *J. Mol. Struct.* **506**, 179–189.
12. Weber, W., V. Helms, J. A. McCammon and P. W. Langhoff (1999) Shedding light on the dark and weakly fluorescent states of green fluorescent proteins. *Proc. Natl. Acad. Sci. U.S.A.* **96**, 6177–6182.
13. Winkler, K. (2002) Ultrafast dynamics in the excited state of green fluorescent protein (wt) studied by frequency-resolved femtosecond pump-probe spectroscopy. *Phys. Chem. Chem. Phys.* **4**, 1072–1081.
14. Litvinenko, K. L. and S. R. Meech (2004) Observation of low frequency vibrational modes in a mutant of green fluorescent protein. *Phys. Chem. Chem. Phys.* **6**, 2012–2014.
15. Hess, S. T., A. A. Heikal and W. W. Webb (2004) Fluorescence photoconversion kinetics in novel green fluorescent protein pH sensors (pHlourins). *J. Phys. Chem. B* **108**, 10138–10148.
16. Brejc, K., T. K. Sixma, P. A. Kitts, S. R. Kain, R. Y. Tsien, M. Ormö and S. J. Remington (1997) Structural basis for dual excitation and photoisomerization of the *Aequorea victoria* green fluorescent protein. *Proc. Natl. Acad. Sci. U.S.A.* **94**, 2306–2311.
17. Kennis, J. T. M., D. S. Larsen, N. H. M. van Stokkum, M. Vengris, J. J. van Thor and R. van Grondelle (2004) Uncovering the hidden ground state of green fluorescent protein. *Proc. Natl. Acad. Sci. U.S.A.* **101**, 17988–17993.
18. Lill, M. A. and V. Helms (2002) Proton shuttle in green fluorescent protein studies by dynamic simulations. *Proc. Natl. Acad. Sci. U.S.A.* **99**, 2778–2781.
19. Stoner-Ma, D., A. A. Jaye, P. Matousek, M. Towrie, S. R. Meech and P. J. Tonge (2005) Observation of excited-state proton transfer in green fluorescent protein using ultrafast vibrational spectroscopy. *J. Am. Chem. Soc.* **127**, 2864–2865.
20. Warren, A. and M. Zimmer (2001) Computational analysis of Thr203 isomerization in green fluorescent protein. *J. Mol. Graph. Model.* **19**, 297–303.
21. Niwa, H., S. Inouye, T. Hirano, T. Matsuno, S. Kojima, M. Kubota, M. Ohashi and F. I. Tsuji (1996) Chemical nature of the light emitter of the *Aequorea* green fluorescent protein. *Proc. Natl. Acad. Sci. U.S.A.* **93**, 13617–13622.
22. Kojima, S., H. Ohkawa, T. Hirano, S. Maki, H. Niwa, M. Ohashi, S. Inouye and F. I. Tsuji (1998) Fluorescent properties of model chromophores of tyrosine-66 substituted mutants of *Aequorea* green fluorescent protein (GFP). *Tetrahedron Lett.* **39**, 5239–5242.
23. Webber, N. M., K. L. Litvinenko and S. R. Meech (2001) Radiationless relaxation in a synthetic analogue of the green fluorescent protein chromophore. *J. Phys. Chem. B* **105**, 8036–8039.
24. Litvinenko, K. L., N. M. Webber and S. R. Meech (2001) An ultrafast polarisation spectroscopy study of internal conversion and orientational relaxation of the chromophore of the green fluorescent protein. *Chem. Phys. Lett.* **346**, 47–53.
25. Martin, M. E., F. Negri and M. Olivucci (2004) Origin, nature, and fate of the fluorescent state of the green fluorescent protein chromophore at the CASPT2//CASSCF resolution. *J. Am. Chem. Soc.* **126**, 5452–5464.
26. Litvinenko, K. L., N. M. Webber and S. R. Meech (2003) Internal conversion in the chromophore of the green fluorescent protein: Temperature dependence and isoviscosity analysis. *J. Phys. Chem. A* **107**, 2616–2623.
27. Mandal, D., T. Tahara, N. M. Webber and S. R. Meech (2002) Ultrafast fluorescence of the chromophore of the green fluorescent protein in alcohol solutions. *Chem. Phys. Lett.* **358**, 495–501.
28. Mandal, D., T. Tahara and S. R. Meech (2004) Excited-state dynamics in the green fluorescent protein chromophore. *J. Phys. Chem. B* **108**, 1102–1108.
29. Kummer, A. D., C. Kompa, H. Niwa, T. Hirano, S. Kojima and M. E. Michel-Beyerle (2002) Viscosity-dependent fluorescence decay of the GFP chromophore in solution due to fast internal conversion. *J. Phys. Chem. B* **106**, 7554–7559.
30. Toniolo, A., S. Olsen, L. Manohar and T. J. Martinez (2004) Conical intersection dynamics in solution: the chromophore of green fluorescent protein. *Faraday Discuss.* **127**, 149–163.
31. Vengris, M., I. H. M. van Stokkum, X. He, A. F. Bell, P. J. Tonge, R. van Grondelle and D. S. Larsen (2004) Ultrafast excited and ground-state dynamics of the green fluorescent protein chromophore in solution. *J. Phys. Chem. A* **108**, 4587–4598.
32. Kwok, W. M., C. Ma, P. Matousek, A. W. Parker, D. Phillips, T. W. T., M. Towrie and S. Umapathy (2001) A determination of the structure of the intramolecular charge transfer state of 4-dimethylaminobenzonitrile (DMABN) by time-resolved resonance Raman spectroscopy. *J. Phys. Chem. A* **105**, 984–990.
33. Maroncelli, M. and G. R. Fleming (1987) Picosecond solvation dynamics of coumarin 153: the importance of molecular aspects of solvation. *J. Chem. Phys.* **86**, 6221–6239.

34. Bublitz, G., B. A. King and S. G. Boxer (1998) Electronic structure of the chromophore in green fluorescent protein (GFP). *J. Am. Chem. Soc.* **120**, 9370–9371.
35. Fleming, G. R. and M. H. Cho (1996) Chromophore-solvent dynamics. *Annu. Rev. Phys. Chem.* **47**, 109–134.
36. Maroncelli, M. (1993) The dynamics of solvation in polar liquids. *J. Mol. Liq.* **57**, 1–37.
37. Castner, E. W. J. and M. Maroncelli (1998) Solvent dynamics derived from optical Kerr effect, dielectric dispersion, and time resolved Stokes shifts measurements: an empirical comparison. *J. Mol. Liq.* **77**, 1–36.
38. Ghose, M., S. Mandal, D. Roy, R. K. Mandal and G. Basu (2001) Dielectric relaxation in a single tryptophan protein. *FEBS Lett.* **509**, 337–340.
39. Cohen, B. E., T. B. McAnaney, E. S. Park, Y. N. Jan, S. G. Boxer and L. Y. Jan (2002) Probing protein electrostatics with a synthetic fluorescent amino acid. *Science* **296**, 1700–1703.
40. Pal, S. K., D. Mandal, D. Sukul, S. Sen and K. Bhattacharyya (2001) Solvation dynamics of DCM in human serum albumin. *J. Phys. Chem. B* **105**, 1438–1441.
41. Changenet-Barret, P., C. T. Choma, E. F. Gooding, W. F. Degrado and R. M. Hochstrasser (2000) Ultrafast dielectric response of proteins from dynamics Stokes shifting of coumarin in calmodulin. *J. Phys. Chem. B* **104**, 9322–9329.
42. Lampa-Pastirk, S. and W. F. Beck (2004) Polar solvation dynamics in Zn(II)-substituted cytochrome c: diffusive sampling of the energy landscape in the hydrophobic core and solvent-contact layer. *J. Phys. Chem. B* **108**, 16288–16294.
43. Jordanides, X. J., M. J. Lang, X. Y. Song and G. R. Fleming (1999) Solvation dynamics in protein environments studied by photon echo spectroscopy. *J. Phys. Chem. B* **103**, 7995–8005.
44. Boyé, S., H. Krogh, I. B. Nielsen, S. B. Nielsen, S. U. Pedersen, U. V. Pedersen, L. H. Andersen, A. F. Bell, X. He and P. J. Tonge (2003) Vibrationally resolved photoabsorption spectroscopy of red fluorescent protein chromophore anions. *Phys. Rev. Lett.* **90.**
45. Van Thor, J. J., T. Gensch, K. J. Hellingwerf and L. N. Johnson (2002) Phototransformation of green fluorescent protein with UV and visible light leads to decarboxylation of glutamate 222. *Nat. Struct. Biol.* **9**, 37–41.
46. Kennis, J. T. M., D. S. Larsen, K. Ohta, M. T. Facciotti, R. M. Glaeser and G. R. Fleming (2002) Ultrafast protein dynamics of bacteriorhodopsin probed by photon echo and transient absorption spectroscopy. *J. Phys. Chem. B* **106**, 6067–6080.
47. Creemers, T. M. H., A. J. Lock, V. Subramaniam, T. M. Jovin and S. Völker (1999) Three photoconvertible forms of green fluorescent protein identified by spectral hole-burning. *Nat. Struct. Biol.* **6**, 557–560.
48. Bell, A. F., X. He, R. M. Wachter and P. J. Tonge (2000) Probing the ground state structure of the green fluorescent protein chromophore using Raman spectroscopy. *Biochemistry* **39**, 4423–4431.
49. Schellenberg, P., E. Johnson, A. P. Esposito, P. J. Reid and W. W. Parson (2001) Resonance Raman scattering by the green fluorescent protein and an analogue of its chromophore. *J. Phys. Chem. B* **105**, 5316–5322.